Chemical Science

Accepted Manuscript

This article can be cited before page numbers have been issued, to do this please use: Q. Yang, X. Yu, E. Lapsheva, P. Pandey, P. W. Smith, H. Gupta, M. Gau, P. Carroll, S. Minasian, J. Autschbach and E. J. Schelter, *Chem. Sci.*, 2025, DOI: 10.1039/D5SC03222A.

ROYAL SOCIETY OF CHEMISTRY

rsc.li/chemical-science

View Article Online
DOI: 10.1039/D5SC03222A

ARTICLE

Comparison of Ce(IV)/Th(IV)-Alkynyl Complexes, and Observation of a *Trans*-Influence Ligand Series for Ce(IV)

Received 00th January 20xx,
Accepted 00th January 20xx

DOI: 10.1039/x0xx00000x

Qiaomu Yang,[a,b] Xiaojuan Yu,[c] Ekaterina Lapsheva,[a,d] Pragati Pandey,[a,e] Patrick W. Smith,[f] Himanshu Gupta,[a] Michael R. Gau,[a] Patrick J. Carroll,[a] Stefan G. Minasian,[f] Jochen Autschbach,[c]* and Eric J. Schelter[a,g,h]*

Organometallic cerium(IV) complexes have been challenging to isolate and characterize due to the strongly oxidizing nature of the cerium(IV) cation. Herein, we report the two cerium(IV) alkynyl complexes: [Ce(TriNOx)(C≡C–SiMe$_3$)] (**1-Ce^{TMS}**) and [Ce(TriNOx)(C≡C–Ph)] (**1-Ce^{Ph}**) (TriNOx^{3-} = *tris*(2-*tert*-butylhydroxylaminato)benzylamine), that include terminal alkyne moieties. The isostructural thorium analogue [Th(TriNOx)(C≡C – SiMe$_3$)] (**1-Th^{TMS}**) was also synthesized and compared with **1-Ce^{TMS}** in bond distance, ^{13}C-NMR, vibrational spectra and electronic structure. The Ce–C bond distances were 2.501(3) Å for **1-Ce^{Ph}** and 2.513(5) Å for **1-Ce^{TMS}** on the shorter end of the few reported Ce^{IV}–C single bonds (2.478(3)-2.705(2) Å), and possibly indicating significant Ce 5d- and 4f-orbital involvement. ^{13}C NMR spectroscopy was also consistent with Ce–C covalency, with significantly deshielded resonances ranging from 185-213 ppm. Such ^{13}C NMR shifts demonstrate a strong influence from spin-orbit coupling (SOC) effects, corroborated by computational studies. Raman analysis showed $\nu_{C\equiv C}$ stretching frequencies of 2000 cm^{-1} (**1-Ce^{TMS}**) and 2052 cm^{-1} (**1-Ce^{Ph}**), indicating the cerium(IV)-alkynyl interaction, compared to the parent HC ≡ CPh (IR = 2105 cm^{-1}, Raman = 2104 cm^{-1}). L3 edge X-ray absorption measurements revealed a predominant Ce(IV) electronic configuration, and magnetic measurements revealed temperature-independent paramagnetism. Electrochemical studies similarly revealed the electron donating ability of the alkynyl ligands, stronger than either fluoride or imido ligands for the Ce(IV)(TriNOx)-framework, with a cerium(IV/III) reduction potential of E_{pc} = −1.58 to −1.66 V vs Fc/Fc$^+$. Evidence for a *trans*-influence has been observed by evaluating a series including previously reported [Ce^{IV}(TriNOx)X]$^{+/0}$ complexes with axial ligands X = THF, I$^-$, Br$^-$, Cl$^-$, F$^-$, $^-$C≡C-Ph, $^-$C≡C-SiMe$_3$, $^-$NH(3,5-(CF$_3$)$_2$-Ar), $^-$OSiPh$_3$, $^-$N(M(L))(3,5-(CF$_3$)$_2$-Ar) [M(L) = Li(TMEDA), K(DME)$_2$ or Cs(2,2,2-crypt)]. These data stand in contrast with previous reports of an inverse *trans*-influence at cerium(IV) and point to differences in involvement of cerium 4f-versus 5d-orbitals in the electronic structures of the complexes.

Introduction

The bonding interactions between f-block elements and organic fragments are of significant interest due to often complex 4f/5f- and 5d/6d-orbital involvement resulting in variable, partially covalent metal-ligand interactions.[1-5] Modern spectroscopic and computational techniques have contributed fruitful studies on this topic.[6, 7] Such studies help to delineate the similarities and differences between bonding in lanthanide, actinide, and d-block metal compounds for applications in reactivity, separations chemistry, and others.[4, 8-10] A key venue for exploring f-/d-bond covalency is the study of high oxidation state compounds, where the high charge on the metal cation can promote orbital overlap with varied contributions from the 4/5f- and 5/6d-manifolds. Such studies require attaining stable complexes in high oxidation states with spectroscopically active ligands for study.[6, 11] In lanthanide chemistry, the most accessible element in this context is cerium(IV). Our group, along with others, has devoted effort to realizing organometallic compounds featuring Ce(IV)–carbon bonds. These studies explore the redox properties and spectroscopic features, together with electronic structure calculations, to model the unique physicochemical signatures and analysis of f-element bond covalency.[1, 2, 12-18]

Organo-cerium(IV) complexes are generally rare,[2] and their scarcity is likely due to redox chemistry, with carbanions prone

[a] *P. Roy and Diana T. Vagelos Laboratories, Department of Chemistry, University of Pennsylvania, 231 S. 34th St., Philadelphia, PA 19104 (USA)*
[b] *Current address: 9700 S. Cass Avenue, The Center of Nanoscale Materials, Argonne National Lab, IL 60439 (USA)*
[c] *732 Natural Sciences Complex, Department of Chemistry, University of Buffalo, Buffalo, NY 14260 (USA)*
[d] *Current address: 410 Forest Ave, Sheboygan Falls, Ereztech Labs, WI 53085*
[e] *Current address: Group of Coordination Chemistry, Institut des Sciences et Ingénierie Chimiques, École Polytechnique Fédérale de Lausanne (EPFL), CH-1015 Lausanne, Switzerland*
[f] *1 Cyclotron Rd, Lawrence Berkeley National Laboratory, Berkeley, CA 94720*
[g] *Department of Chemical and Biomolecular Engineering, University of Pennsylvania, 220 S. 33rd St., 311A Towne Building, Philadelphia, PA, 19104 (USA)*
[h] *Department of Earth and Environmental Science, University of Pennsylvania, 251 Hayden Hall, 240 South 33rd Street, Philadelphia, PA 19104 (USA)*

Supplementary Information available: [details of any supplementary information available should be included here]. See DOI: 10.1039/x0xx00000x

View Article Online DOI: 10.1039/D5SC03834A

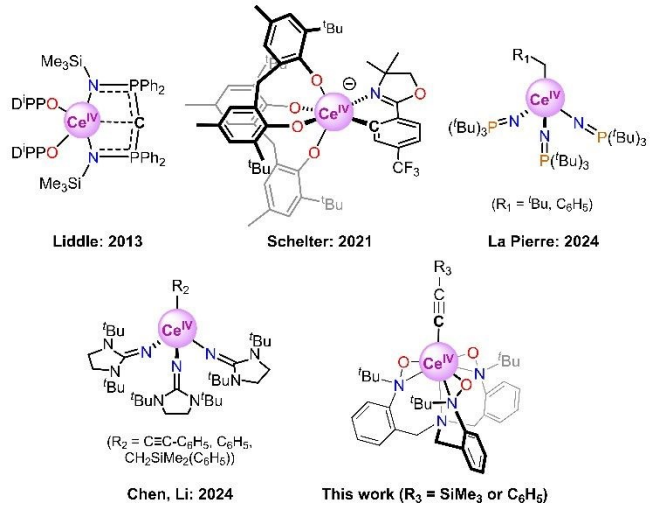

Fig. 1 Recent examples of cerium(IV)-carbon containing complexes, including heteratom-stabilized Ce(IV) compounds, or Ce(IV) complexes with monodentate carbanion ligands.

to oxidation and cerium(IV) cations prone to reduction. Notable examples in the field include the metallocene Ce(IV) complexes, heteroatom-stabilized Ce(IV)-C compounds, and Ce(IV) complexes with monodentate, carbanion ligands. Metallocene complexes include cerium(IV) cyclopentadienides,[19, 20] cerium(IV) cyclooctatetraenes such as $[Ce(COT)_2]$,[15, 21-23] or cerium(IV) bispentalenides, with important examples reported between 1976 to 2010.[24] Progress has also been made in heteroatom-stabilized cerium(IV)-carbon complexes. P. Arnold and coworkers reported the use of *N*-heterocyclic carbene ligand featuring Ce^{IV}-C_{sp2} bond in 2009,[25] and Liddle and coworkers studied the bis(iminophophorano)methandiide (BIPM) ligand in $[Ce^{IV}(BIPM^{TMS})_2]$ featuring Ce^{IV}-C_{sp2} bond in 2013 (Figure 1).[3, 14] Our group reported $[Ce^{IV}(\kappa^2\text{-ortho-oxa})(MBP)_2]^-$ in 2021,[2] where ortho-oxa = dihydrodimethyl-2-[4-(trifluoromethyl)phenyl]-oxazolide, MBP = 2,2'-methylenebis(6-tert-butyl-4-methylphenolate). The complex featured a Ce^{IV}-aryl (C_{sp2}) bond supported by a chelating oxazolide group. Recent progress has been made in Ce-C single bond chemistry, without supporting chelating groups using monodentate supporting ligands. Chen, Li, Tamm, *et al.* recently used the imidazolin-2-iminato (ImN^-) ligand featuring a Ce^{IV}-alkynyl (C_{sp}) bond in $[Ce^{IV}(C\equiv C\text{-Ph})(ImN)_3]$ complexes in 2024.[26] In the same work, the team also realized compounds featuring Ce^{IV}-aryl (C_{sp2}) and Ce^{IV}-alkyl (C_{sp3}) bonds. Independently and at the same time, La Pierre and and co-workers have employed the tri-*tert*-butyl imidophosphorane ligand on $[Ce^{IV}(Alkyl)(NP(tert\text{-}butyl)_3)_3]$ featuring Ce^{IV}-alkyl (C_{sp3}) bonds, where Alkyl is neopentyl (Npt) or benzyl (Bn).[27] And a Ce^{IV}-cyclopropenyl complex featuring Ce^{IV}-C_{sp2} bond and ring-open isomerization was recently disclosed by us.[28]

In pursuit of cerium(IV) organometallic complexes, three primary synthetic strategies have been employed: the use of a supporting ligand with electron-donating groups to otherwise stabilize the Ce^{IV} oxidation state; the use of multidentate ligands with both a carbanion and electronically-supporting heteroatoms coordinating to the Ce^{IV} cation, and tethering of ligands with steric bulk to kinetically inhibit the homolysis of the Ce^{IV}-C bond.[2] In this study, we sought to employ the first strategy to further expand the scope of Ce^{IV}-C chemistry and realize Ce^{IV}-alkynyl complexes. The $TriNOx^{3-}$ ligand has been used by us for the stabilization of the Ce(IV) oxidation state and a series of $[Ce^{IV}(TriNOx)X]^{+/0}$ axial complexes, X = THF, I^-, Br^-, Cl^-, F^-,[29] anilide,[12] imide,[6, 12, 13, 30] siloxide,[13] carbamate,[30] and oxo,[6, 13] have been synthesized previously. For the current work, H-C≡C-$SiMe_3$ and H-C≡C-Ph have been used as two alkyne precursors. As a result, compounds with Ce^{IV}-C_{sp} bonds were obtained without heteroatom stabilization and without steric hindrance provided by bulky substituents. This approach also provided the opportunity for a more direct analysis of the cerium(IV)-carbon bonding interactions without the influence of conjugated heteroatoms.

Herein, we report the isolation of Ce(IV)-C_{sp} compounds with terminal carbon atom coordination (Figure 1). The complexes provide opportunities for spectroscopic characterization of the –C≡C– vibrations and electronic structure calculations. The observed ^{13}C NMR chemical shifts of the title compounds are remarkably downfield because of effects originating from a spin-orbit interaction. The alkynyl moiety is also found to be a strong donor for stabilizing cerium(IV) with metal redox potentials of −1.49 and −1.57 V vs Fc/Fc^+ ($Fc=Fe(C_5H_5)_2$). The information obtained in the present study has been applied to complete a *trans* influence series for related $[Ce^{IV}(TriNOx)X]^{+/0}$ complexes with axial ligands X including THF, halide, alkynyl, amide, siloxide, and imide ligands. These results provide important opportunities for improving our understanding of the bonding involving lanthanides in high oxidation states.

Results and Discussion

Synthesis of Cerium(IV) and Thorium(IV) Alkynyl Complexes

The precursor complex $[Ce^{IV}(TriNOx)Cl]$ (**1-Ce^{Cl}**) was obtained by mixing $[Ce^{III}(TriNOx)(THF)]$ with CPh_3Cl in Et_2O in a modified reaction based on previous reports,[29] where the purple solid

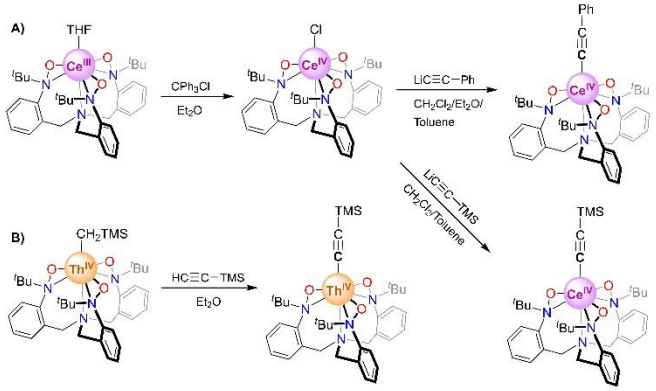

Fig. 2 Syntheses of **A)** Ce^{IV}-alkynyl complexes (**1-Ce^{Ph}** and **1-Ce^{TMS}**) and **B)** Th^{IV}-alkynyl complex (**1-Th^{TMS}**).

View Article Online
DOI: 10.1039/D5SC03222A

product precipitates immediately, with a simple workup and high (90%) yield. Addition of a dark purple solution of [Ce(TriNOx)Cl] in CH_2Cl_2 to a colorless solution of Li-C≡C-Ph (1.6 equiv) in a toluene/Et_2O (1:1) mixture resulted in a cloudy maroon colored solution of [Ce(TriNOx)(C≡C-Ph)] (**1-Ce^{Ph}**, see Figure 2A). The use of 1.6 equiv Li-C≡C-Ph was based on empirical observation and used to ensure complete formation of the product **1-Ce^{Ph}**. The solvent was stripped under reduced pressure and the resulting solid was washed by Et_2O to afford the pure product of **1-Ce^{Ph}** in 80% yield. Maroon X-ray quality crystals were grown from a cooled (−25 °C) solution of **1-Ce^{Ph}** in fluorobenzene with pentane diffusion over 2 d. Complex [Ce(TriNOx)(C≡C-TMS)] (**1-Ce^{TMS}**) was obtained in 64% yield, following a similar procedure where pure toluene was used as the solvent instead of a toluene/Et_2O mixture. Dark maroon X-ray quality crystals of **1-Ce^{TMS}** were grown from a cooled (−25 °C) solution of toluene with pentane diffusion over 3 d. **1-Ce^{TMS}** and **1-Ce^{Ph}** exhibit different solubilities; the former is soluble in Et_2O or toluene and the latter is not. A thorium(IV) analogue was synthesized by addition of a HC≡C-$SiMe_3$ solution in Et_2O to a colorless solution of [Th(CH_2SiMe_3)(TriNOx)] in Et_2O dropwise, resulting in a white cloudy solution (see Figure 2B). Complex [Th(TriNOx)(C≡C-$SiMe_3$)] (**1-Th^{TMS}**) was obtained in 50% yield following filtration and washing the precipitate with Et_2O. X-ray quality colorless crystals of **1-Th^{TMS}** were similarly grown from a cooled (−25 °C) solution of toluene/dichloromethane with pentane diffusion over 3 d.

X-ray Structures of 1-Ce^{Ph}, 1-Ce^{TMS}, and 1-Th^{TMS}

X-ray crystallography experiments confirmed the structures of **1-Ce^{Ph}** and **1-Ce^{TMS}** featuring the –C≡C–R (–R = –Ph or –$SiMe_3$) moiety in the axial position of the $[Ce^{IV}(TriNOx)]^+$ complex. The Ce–C bond distances were 2.501(3) Å for **1-Ce^{Ph}** and 2.513(5) Å for **1-Ce^{TMS}** (Figure 3). The slightly shorter bond distance in **1-Ce^{Ph}** is consistent with computational results, *vide infra*.

Table 1. Cerium-carbon distance (Å), including literature value and our examples.

Bond Type	Bond Distance (Å)	Reference
Ce^{III}–$C_{cyanide}$	2.596(15)–2.736(17)	(31)
Ce^{III}–$C_{alkynyl}$	2.549(3)–2.71(2)	(32)
Ce^{III}–$C_{alkynyl}$	2.652(9)	(33)
Ce^{IV}–$C_{carbene}$	2.652(7)-2.705(2)	(25)
Ce^{IV}–C_{aryl}	2.571(7)-2.5806(19)	(2)
Ce^{IV}–C_{aryl}	2.539(3)	(26)
Ce^{IV}–C_{alkyl}	2.515(4)	(26)
Ce^{IV}–C_{alkyl}	2.508(2)-2.562(2)	(27)
Ce^{IV}–$C_{alkynyl}$	2.478(3)-2.523(10)	(26)
Ce^{IV}–$C_{alkynyl}$	2.513(5)	**1-Ce^{Ph}**
Ce^{IV}–$C_{alkynyl}$	2.501(3)	**1-Ce^{TMS}**
Ce^{IV}–$C_{heter\text{-}atom\ supported\ multiple\ bond}$	2.385(2)-2.441(5)	(14)

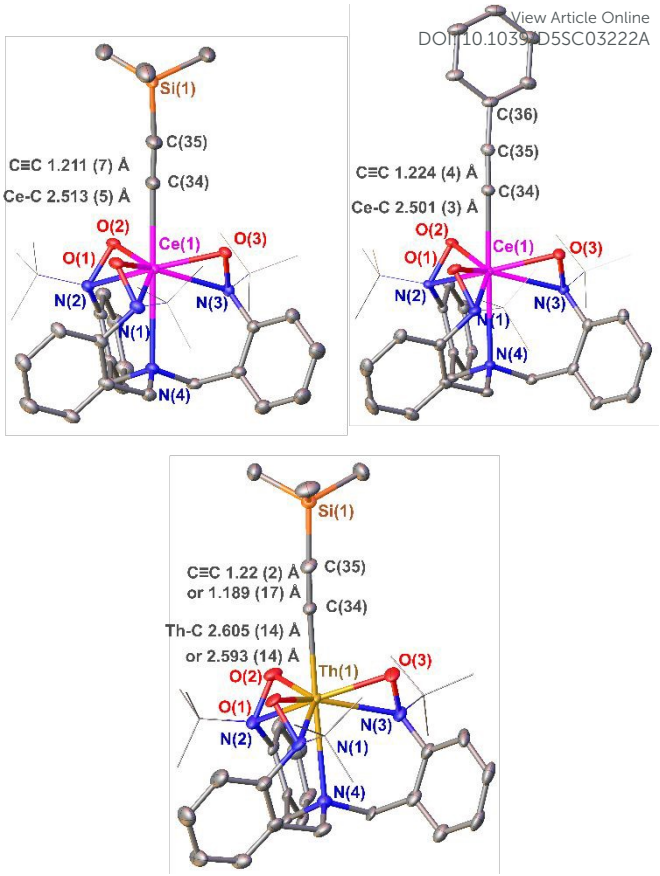

Fig. 3 X-ray crystal structures of **1-Ce^{TMS}**, **1-Ce^{Ph}** and **1-Th^{TMS}**. Thermal ellipsoids were plotted at 30% probability level. For clarity, hydrogens and solvent molecules in the crystal structure are omitted; *tert*-butyl groups are displayed in wireframe.

These Ce^{IV}–C_{sp} bond distances are shorter than those previously reported Ce^{III}–C_{sp} in cerium-cyanide complexes (2.596(15)–2.736(17) Å),[31] such as $[N^nBu_4]_2[(C_5Me_5)_2Ce^{III}(CN)_3]$); alkynyl complexes (2.549(3)–2.71(2) Å),[32] such as $[(C_5Me_5)_2Ce(CC^tBu)_2Li(THF)]$; and a cerium(III) phenolate alkynyl complex (2.652(9) Å),[33] Na[Ce(CCPh)(bdmmp)$_3$] (bdmmp = 2,6-bis-(dimethylamino)-4-methylphenolate). The shorter distances of the Ce^{IV}–C_{sp} bonds in **1-Ce^{Ph}** and **1-Ce^{TMS}** are consistent with the ~0.1 Å smaller ionic radius of the cerium(IV) ion compared to cerium(III) with similar coordination numbers.[34] The interatomic distance has been summarized into a table (see **Table 1** and supporting information).

These Ce^{IV}–C_{sp} bond distances are also shorter than previously reported single Ce^{IV}–C bonds in Ce^{IV} *N*-heterocyclic carbene complexes (2.652(7)-2.705(2) Å),[25] such as $Ce^{IV}[OCMe_2CH_2(1\text{-}C\{NCHCHN^iPr\})]_4$; Ce^{IV} oxazolide aryl complex (2.571(7)-2.5806(19) Å),[2] such as $[Li(DME)_3][Ce^{IV}\{\kappa^2\text{-dihydrodimethyl-2-[4-(trifluoromethyl)phenyl]-oxazolide}\}(2,2'\text{-methylenebis(6-tert-butyl-4-methylphenolate)}_2$; Ce^{IV} tris(imidazoline-2-iminato) alkyl complex (2.515(4) Å) and aryl complex (2.539(3) Å);[26] Ce^{IV} imidophosphorane alkyl complex (2.508(2)-2.562(2) Å),[27] such as Ce^{IV} benzyl tris(tri-tert-butyl imidophosphorane). But our Ce^{IV}-C_{sp} bond distances are similar to the Ce^{IV}-C bond in Ce^{IV} tris(imidazoline-2-iminato) alkynyl complex (2.478(3)-2.523(10)

View Article Online
DOI: 10.1039/D5SC03222A

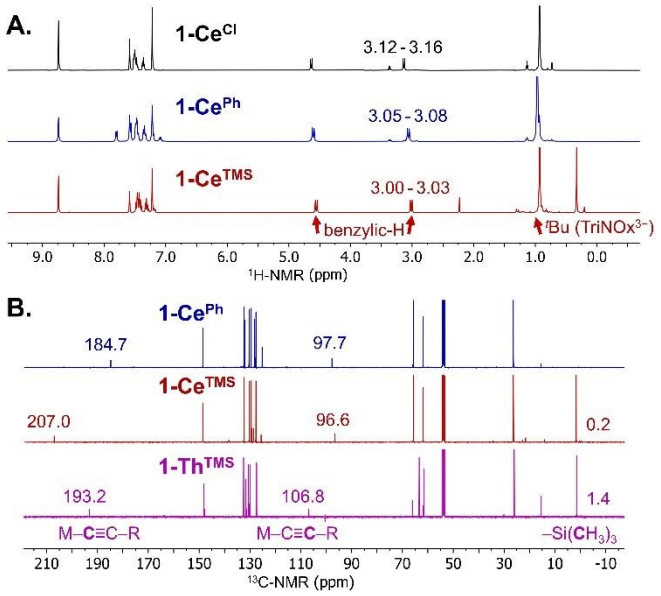

Fig. 4 A) ^{1}H-NMR spectra for **1-Ce^{Cl}**, **1-Ce^{Ph}** and **1-Ce^{TMS}** recorded in pyridine-d_5. The spectrum of **1-Ce^{TMS}** includes peaks for residual toluene after crystallization and drying. B) ^{13}C-NMR spectra for **1-Ce^{Ph}**, **1-Ce^{TMS}** and **1-Th^{TMS}** in CD_2Cl_2.

Å),[26] and are longer than the Ce^{IV} and carbon bond in the heteroatom-supported bis(iminophosphorano)methandiide complex (2.385(2)-2.441(5) Å),[14] such as Ce{C[PPh$_2$N(SiMe$_3$)]}[O(2,6-diisopropylphenyl)]$_2$ (Figure 1). The short Ce^{IV}–C$_{sp}$ distances possibly indicates appreciable cerium(IV)-carbon interactions, especially considering that the coordination of the alkynyl moieties to the cerium is unsupported in the case of the compounds reported here.

X-ray crystallography experiments confirmed the molecular structure of related **1-Th^{TMS}** was isostructural to **1-Ce^{TMS}**. There are two independent molecules of **1-Th^{TMS}** in the asymmetric unit with minor differences, with the Th–C$_{sp}$ bond distances of 2.593(14) and 2.605 (14) Å. Thorium(IV)-alkynyl complexes have been reported previously,[35-39] where the reported Th^{IV}–C bond lengths ranged from 2.450(7) to 2.642(5) Å. The Th^{IV}–C bond distance in **1-Th^{TMS}** is similar or slightly longer than these literature values, likely due to the electron-donating TriNOx^{3-} ligand. This bond length in **1-Th^{TMS}** is also 0.086 Å longer than the Ce–C distance in **1-Ce^{TMS}**, consistent with a slight larger ionic radius of thorium(IV) of 1.05 Å, than cerium(IV) of 0.97 Å, with an oxidation state of +4 and coordination number of 8.[34]

NMR Spectroscopy and Computational Studies

Consistent with our previous work,[29] the solution ^{1}H-NMR spectra of the complexes studied here indicated C_{3v} symmetry of TriNOx^{3-} ligand framework with diastereotopic benzylic protons (CH$_2$). Complex **1-Ce^{Ph}** exhibits –CH$_2$ resonances at 4.62–4.59, 3.08–3.05 ppm and a ^{t}Bu resonance at 0.93 ppm, while **1-Ce^{TMS}** exhibits –CH$_2$ resonances at 4.57–4.54, 3.03–3.00 ppm and a ^{t}Bu resonance at 0.97 ppm. The overall chemical shifts were consistent with closed shell complexes for both **1-Ce^{TMS}** and **1-Ce^{Ph}**. Based on the chemical shifts in the ^{1}H-NMR spectra and cerium-carbon bond distances, we assigned **1-Ce^{TMS}** and **1-Ce^{Ph}** as Ce^{IV} complexes.

We also observed previously that the ^{1}H-NMR chemical shifts of the diastereotopic benzylic resonances (CH$_2$) and *tert*-butyl (^{t}Bu) resonances in the TriNOx^{3-} arms were sensitive to the axial ligand identity. The –CH$_2$ and –^{t}Bu proton resonances were used to differentiate inner- or outer sphere coordination to the [Ce(TriNOx)]$^{+}$ fragment in the solution phase.[29] For example, [Ce(TriNOx)]I exhibits ^{1}H-NMR CH$_2$ resonances between 4.73–4.67 and 4.07–4.03 ppm, and a ^{t}Bu resonance at 0.72 ppm, features that were confirmed as corresponding to an outer-sphere iodide anion. Whereas the [Ce(TriNOx)Cl] complex has an inner-sphere chloride axial ligand in solution with –CH$_2$ proton resonances spanning 4.66–4.62, and 3.16–3.12 ppm and characteristic and ^{t}Bu resonance at 0.94 ppm. In particular, the larger differences in the diastereotopic –CH$_2$ chemical shift ranges were correlated with the geometry difference between inner- and outer axial ligand coordination. For the current work, the chemical shifts of **1-Ce^{Ph}** and **1-Ce^{TMS}** resemble the inner-sphere [Ce(TriNOx)Cl] at around 3.1 and 0.9 ppm (Figure 4A). Thus, the chemical shift indicates, as expected, that the alkynyl is coordinated to the cerium(IV) cation in solution, consistent with the result from cyclic voltammetry, *vide infra*. The thorium(IV) alkynyl complex **1-Th^{TMS}** resembles the cerium analogues **1-Ce^{TMS}** in C_6D_6 (See Supplementary Information), and was also assigned as an inner-sphere alkynyl complex.

Considering the ^{1}H-NMR resonances of **1-Ce^{Ph}** and **1-Ce^{TMS}** it was noteworthy that the upfield chemical shift of the –CH$_2$ signals corresponded to a relatively stronger bonding interaction of the axial ligand with the cerium(IV) cation. The trend was noted by us previously for [Ce(TriNOx)Br] (4.71–4.62, 3.34–3.30 ppm), [Ce(TriNOx)Cl] (4.66–4.62, 3.16–3.12 ppm), and [Ce(TriNOx)F] (4.64–4.60, 3.08–3.04 ppm) in pyridine-d_5.[29] In comparison, the –CH$_2$ ^{1}H-NMR resonances for **1-Ce^{Ph}** (4.62–4.59, 3.08–3.05 ppm) are similar to [Ce(TriNOx)F], while the –CH$_2$ resonance for **1-Ce^{TMS}** (4.57–4.54, 3.03–3.00 ppm) is further upfield. This result indicates the stronger electron donating ability of -C≡C-SiMe$_3$ than -C≡C-Ph for the Ce^{IV} cation, consistent with the cerium(III/IV) electrochemistry results, ^{13}C-NMR spectroscopy results, and the observations of a *trans*-influence for the system (*vide infra*).

After confirming the chemical structures and the ^{1}H-NMR of **1-Ce^{TMS}**, **1-Ce^{Ph}** and **1-Th^{TMS}**, we turned to investigations of ^{13}C-NMR spectra. Atoms directly bound to closed-shell heavy elements, especially actinides, are known to have a characteristically significant downfield shift.[40, 41] This deshielding effect has been correlated to the degree of covalency in the metal-ligand bond.[41-43] The effect has been found, for example, for C$_{sp3}$, C$_{sp2}$ and hydrogen atoms in diamagnetic Th(IV) and U(VI) complexes.[7, 44-48] For thorium, the largest ^{13}C-NMR spectroscopy chemical shift δ 230.8 ppm was observed for Th(2-C$_6$H$_4$CH$_2$NMe$_2$)$_4$,[48] while the largest ^{1}H-NMR chemical shift was estimated by DFT calculations at 20.3 ppm for ThH[N(SiMe$_3$)$_2$]$_3$.[49] Recent progress in obtaining isolable

View Article Online
DOI: 10.1039/D5SC03223A

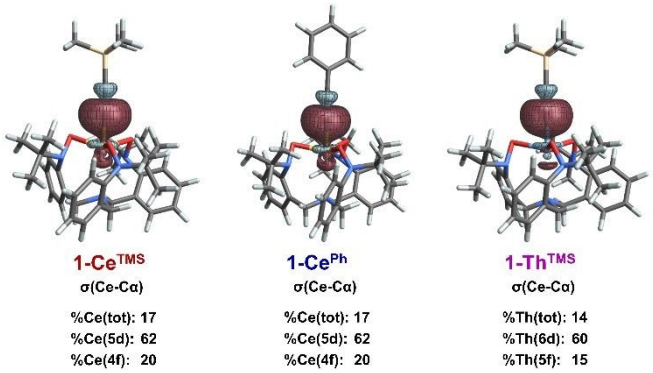

Figure 5. Isosurfaces (±0.03 a.u.) of the σ(Ce–C_α) bonding NLMOs in **1-Ce^{TMS}**, **1-Ce^{Ph}**, and **1-Th^{TMS}**, along with total weight-% metal character and 6d vs. 5f contributions at the metal. (Color code: Ce yellow, Th sky blue, Si wheat, C gray, O red, N blue, H white.)

cerium(IV)-carbon bonded complexes has demonstrated similar downfield shifts as in actinide compounds,[2, 3, 14, 25] where the largest chemical shift of ^{13}C was δ 343.5 ppm was observed for $Ce^{IV}[C(Ph_2PNSiMe_3)_2]_2$ complex.[3] Notably, this cerium(IV) complex had the Ce-C bond supported by heteroatom coordination and conjugation, including two phosphorous atoms bound at the central carbon, qualifying a direct comparison.

In the current cases (Figure 4B), the ^{13}C chemical shifts are 184.7 ppm for **1-Ce^{Ph}** in CD_2Cl_2 and 207.0 ppm for **1-Ce^{TMS}** in CD_2Cl_2 (and 213.0 ppm in C_6D_6), well outside the typical range for alkynyl resonances (65–90 ppm).[50] Thus, the strong downfield shift indicated potentially a large spin-orbit coupling contribution to the chemical shift, as with other cerium(IV)-carbon moieties.[7] This observation also reflects the strong cerium-alkynyl bonding interactions. The [Ce(TriNOx)(**C**≡C-Ph)] has a larger ^{13}C-NMR shifts at 184.7 ppm than those reported in the Ce^{IV}-C_{sp} complex [Ce^{IV}(ImN)$_3$(**C**≡C-Ph)] at 176.4 ppm by Chen and Li. It should be noted that these ^{13}C-NMR shifts are smaller than those reported in the Ce^{IV}–C_{aryl} complex (255.6 ppm for cerium oxazolide complex) by us previously.[2] This is presumably because the $^{13}C_{sp2}$-NMR chemical shift (100–170 ppm for arenes),[2] is intrinsically larger than the $^{13}C_{sp}$-NMR chemical shift (60-100 ppm for alkynes).

To understand the Ce^{IV}/Th^{IV}-C bonding interactions and the influence of spin-orbit coupling, computational analyses were carried out, including calculations of the carbon NMR chemical shifts. Density functional theory (DFT) calculations were initially performed for **1-Ce^{TMS}**, **1-Ce^{Ph}**, and **1-Th^{TMS}** using the B3LYP hybrid functional. Complete computational details are provided in the Supporting Information. B3LYP is frequently used for molecular structure optimizations and bonding studies and therefore we used it for these purposes in the present investigation.[51, 52] Selected optimized bond distances of **1-Ce^{TMS}**, **1-Ce^{Ph}**, and **1-Th^{TMS}** are compared to the experimental crystal structure data in Table S3. The optimized M–C bond metrics align closely with the experimental data, with deviations of only 0.001 Å and 0.03 Å for the Ce–C and Th–C distances, respectively, confirming the reliability of the chosen computational model.

To explore the nature of the M–C interactions, we employed natural localized molecular orbital (NLMO) analyses to assess the covalency resulting from the σ donation in **1-Ce^{TMS}**, **1-Ce^{Ph}**, and **1-Th^{TMS}**. Relevant orbitals are depicted in Figure 5, and atomic hybrid contributions in the NLMOs and bond order analysis representing the important bonding interactions are listed in Tables S4 and S5. Given the similarity in the bonding characteristic of **1-Ce^{TMS}**, **1-Ce^{Ph}**, we mainly focused on **1-Ce^{TMS}** versus **1-Th^{TMS}**. For **1-Ce^{TMS}**, the NLMO analysis reveals a σ(Ce–C_α) bond with 17% total Ce density weight (18% 6s; 62% 5d; 20% 4f), along with two orthogonal π(C_α–C_β) bonds showing negligible Ce weights (1% each). In other words, there is a Ce—C_α σ bond which is polarized toward carbon. The 17% density weight on Ce means that electron density corresponding to about 0.34 electrons is donated to Ce (the NLMO is doubly occupied). In contrast, the σ(Th–C_α) NLMO for **1-Th^{TMS}** exhibits 14% (60% 6d; 15% 5f) Th weight, i.e., lower than that of the Ce analogue. The calculations therefore indicate that the extent of metal–ligand covalent bonding with the ligands studied herein is greater for Ce(IV)- than Th(IV)-carbon bonds, which is in line with reported data for thorium(IV)-imido versus cerium(IV)-imido complexes from our group.[53] These results and a growing body of evidence suggest that the notion that lanthanide bonding is not covalent is inappropriate.

The ^{13}C NMR chemical shifts for complexes **1-Ce^{TMS}**, **1-Ce^{Ph}** were calculated using a functional designated here as PBE0(40) (a PBE-based hybrid with 40% exact exchange), without and with inclusion of the SO interaction. This functional has previously been shown to accurately predict ^{13}C NMR chemical shifts in organometallic cerium complexes.[2, 54, 55] A summary of calculated shielding constants and chemical shifts is listed in Table S6. The calculated and experimental ^{13}C chemical shifts are in excellent agreement. For example, the calculated C_α shift for **1-Ce^{TMS}** is 207.3 ppm (expt. = 207.0 ppm), which includes a 19.4 ppm deshielding contribution due to SO effects that is primarily attributed to the strong SO coupling within the Ce 4f (and 5d) shell and its involvement in the chemical bond with C_α. For comparison, the calculated C_α shift for **1-Th^{TMS}** is 195.5 ppm (expt. = 193.2 ppm), with a 25.4 ppm shift due to SO coupling. This is consistent with a weaker covalency of thorium compared with cerium, but a larger SO coupling due to heavy element effect. In another comparison, the calculated C_α shift for **1-Ce^{Ph}** is 186.8 ppm (expt. = 184.7 ppm), which includes a 20.4 ppm deshielding from the SO interaction. The similar SOC deshielding in **1-Ce^{Ph}** relative to **1-Ce^{TMS}** commensurate with its similar Ce-C_α bonding covalency.

Vibrational Spectroscopy and Analysis

Bonding interactions of alkynyl moieties with various cationic moieties has been studied by vibrational spectroscopies previously.[56-65] Upon bonding to a metal cation, the metal-

View Article Online
DOI: 10.1039/D5SC03222A

alkynyl (M–C) interaction might be expected to influence the vibrational frequency of the –C≡C– moiety due to metal-alkynyl σ– and π–bonding interactions.[56, 65] For the present study, we have only considered the impact of σ–bonding interactions.

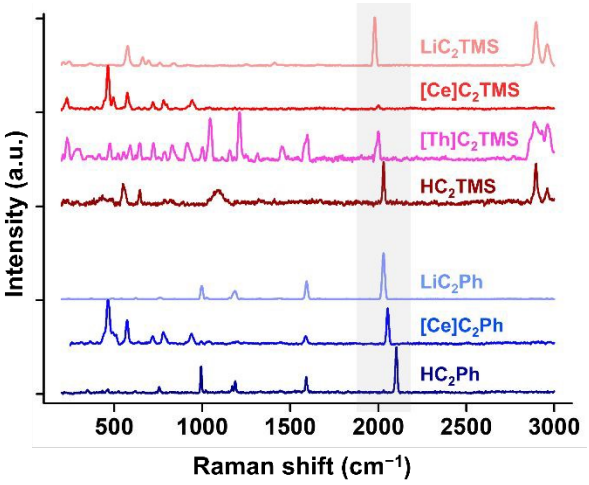

Fig. 6 Raman spectra of **1-Ce^{TMS}**, **1-Ce^{Ph}**, and **1-Th^{Ph}**, and comparison with lithium-acetylide complex and protonated alkyne.

No vibrational spectra of cerium(IV)-alkynyl complexes have previously been reported. Here, we collected the infrared (IR) absorption and Raman spectra of **1-Ce^{TMS}**, **1-Ce^{Ph}**, and **1-Th^{TMS}** to identify the vibrational frequencies of the –C≡C– moiety (Figure 6, and Supporting Information) and compared with other metal-alkynyl complexes. For the M–C≡C-TMS complexes, the observed $\nu_{C\equiv C}$ stretching frequencies were **1-Ce^{TMS}** (Raman = 2000 cm^{-1}), and **1-Th^{TMS}** (Raman = 2003 cm^{-1}). The notably weak Raman signal for **1-Ce^{TMS}** was intrinsic and observed over multiple samples/measurements. The reasons for the lower Raman signal strength are for **1-Ce^{TMS}** compared to for **1-Th^{TMS}** are, as yet, unclear. For M–C≡CPh, **1-Ce^{Ph}** (Raman = 2052 cm^{-1}), was shown to have a $\nu_{C\equiv C}$ stretching frequency that was lower than in HC≡CPh (IR = 2105 cm^{-1}, Raman = 2104 cm^{-1}). Vibrational spectra of related metal-acetylide complexes reported in the literature include Yb(C≡CPh)(C$_5$H$_5$)$_2$ (IR = 2040 cm^{-1}),[63] and Zr(C≡CPh)$_2$(C$_5$Me$_5$)$_2$ (IR = 2073 cm^{-1}).[57] Based on these reported results, the vibrational frequency of the alkynyl moiety reflects the metal-alkynyl σ-bond interactions (Figure S48). We contend that the $\nu_{C\equiv C}$ stretching frequencies for **1-Ce^{TMS}**, **1-Ce^{Ph}**, and **1-Th^{TMS}** are approximately intermediate between those observed for the more purely ionic f-block (low frequency) and relatively more covalent d-block (high frequency) metal congeners.[1, 16, 21]

Magnetometry, L_3-Edge X-ray Absorption Spectroscopy and UV-Vis Absorption Spectroscopy

The short Ce–C bonds, downfield ^{13}C chemical shifts, negative reduction potentials and characteristic $\nu_{C\equiv C}$ stretching frequencies highlighted the interactions between cerium metal and alkynyl ligands in **1-Ce^{TMS}** and **1-Ce^{Ph}**. These complexes present an opportunity for further study, as the unfilled low-lying 4f-orbitals in cerium(IV) can result in multi-configurational ground states in some cases.[6, 66]

The Ce L_3-edge (Ce 2p → 5d) X-ray absorption near edge structure (XANES) spectra of **1-Ce^{TMS}** and **1-Ce^{Ph}** are shown in Figure S56-S57. A characteristic double-peaked structure is observed, which is attributed to excitations of the core hole electron (2p) to 4f$^1\underline{L}$ 5d^1 and 4f^{0}5d^1 final states, where $\underline{L}$ indicates a hole (vacancy) at the ligand.[6, 17] The intensities of both peaks were evaluated using established curve-fitting methods, which indicated that the weight of the 4f^{0}5d^1 configuration had statistically equivalent values for both complexes, with relative weights of 0.43(3) for **1-Ce^{TMS}** and 0.46(3) for **1-Ce^{Ph}**. These configuration weights are comparable to other cerium(IV) complexes, such as cerium(IV) TriNOx^{3-} imido complexes (0.37(3)-0.45(3)),[6] and cerium(IV) TriNOx^{3-} oxo complexes (0.39(3)-0.41(3)).[6] Although fitting was unable to quantify any difference, visual inspection of the normalized spectra shows that the feature at higher energy is more intense for **1-Ce^{Ph}**. We reach the qualitative determination that the 4f electron density at Ce is lower for **1-Ce^{Ph}** relative to **1-Ce^{TMS}**.

Having evaluated the amount of charge transfer for **1-Ce^{TMS}** and **1-Ce^{Ph}**, we next turned to temperature dependent magnetic studies of the compounds. Van Vleck temperature-independent paramagnetism (TIP) has been observed for molecular, formally cerium(IV) complexes,[6, 66-68] arising from small energy differences between the open-shell singlet ground state and admixed, low-lying triplet excited states.[67] Magnetometry studies were carried out on **1-Ce^{Ph}**. The variable field magnetization was collected for **1-Ce^{Ph}** at 2 K, which shows the presence of a negligible magnetic impurity that saturates below M < 0.01 μB (Figure S52), and indicating the +IV oxidation state of cerium in **1-Ce^{Ph}**. Variable temperature magnetic susceptibility for **1-Ce^{Ph}** was collected at 1.0 T applied field (Figure S53, S54). The susceptibility plot of χT vs T shows a linear decrease from high (300 K) to low temperature (2 K). After accounting for the intrinsic diamagnetic contribution using Pascal's constants, the TIP value for this cerium(IV) complex was determined to be 6.34(1)×10^{-4} emu mol^{-1}. This value is similar to, or larger than, reported cerium(IV) complexes such as cerocene (1.4(2)×10^{-4} emu mol^{-1}),[68] [NEt$_4$]$_2$[CeCl$_6$] (1.6(2)×10^{-4} emu mol^{-1}),[66] [K(DME)$_2$][Ce(TriNOx)(=NAr^F)] (2.2(2)×10^{-4} emu mol^{-1}).[6] UV-Vis absorption spectra were taken for both **1-Ce^{TMS}** and **1-Ce^{Ph}**, where **1-Ce^{TMS}** showed a peak at 358 nm, and **1-Ce^{Ph}** showed a peak at 382 nm, and both were attributed to LMCT (Figure S50). Overall, our experimental data confirm pure cerium(IV) oxidation states and reveal the electronic structure and configuration for the cerium-alkynyl complex.

Electrochemical Studies

To better understand the impact of the alkynyl group on the stabilization of the cerium(IV) ion, electrochemical studies were performed on **1-Ce^{Ph}** and **1-Ce^{TMS}** to measure the potential of the Ce(III/IV) redox couple. The electrochemical properties of

View Article Online DOI: 10.1039/D5SC07223A

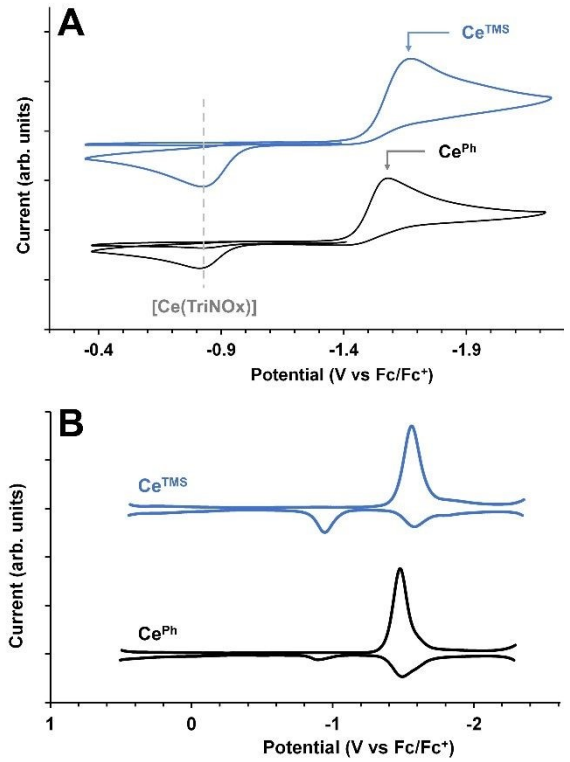

Fig. 7 A) Cyclic voltammograms (CVs) of **1-Ce^{TMS}** and **1-Ce^{Ph}** (3 mM) in CH_2Cl_2 using [$^nPr_4N$][BAr^F_4] (100 mM) as the supporting electrolyte. Scan Rate: 100 mV/s. All sweeps were perfoemd in the oxidative direction. The trace shows reduction features for **1-Ce^{TMS}** (E_{pc} = −1.66 V) and **1-Ce^{Ph}** (E_{pc} = −1.58 V), followed by an oxidation feature at E_{pa} = −0.82/−0.81 V, the latter of which do not appear in the first scan. B) Differential Pulse Voltammagrams (DPV) of **1-Ce^{TMS}** and **1-Ce^{Ph}**.

[Ce^{IV}(TriNOx)X] have been studied previously to identify the solution speciation and compare the redox potentials, where X^- = F^-, Cl^-, Br^-, I^-, OTf^- (OTf^- = $CF_3SO_2O^-$), or [NAr^F][$M(L)_x$]$^-$ (Ar^F = 3,5-$(CF_3)_2$-C_6H_3; M = Li, K, Rb, or Cs; L = THF, TMEDA, DME, or 2.2.2-cryptand, x = 1 or 2). The previously reported redox potentials of the [Ce^{IV}(TriNOx)]$^+$ framework were in accord with the electron-donating character of the axially coordinated moieties. For example, the potentials of the reduction waves versus Fc/Fc^+ of the Ce(IV) compounds with axial ligands ranging from weakly donating to strongly donating ligand are: [Ce(TriNOx)][OTf] (E_{pc} = −1.04 V), [Ce(TriNOx)Br] (E_{pc} = −1.04/−1.16 V), [Ce(TriNOx)Cl] (E_{pc} = −1.26 V), [Ce(TriNOx)F] (E_{pc} = −1.40 V) and [$M(L)_x$][Ce(TriNOx)=N-Ar] (-Ar = -(3,5-$(CF_3)_2C_6H_3$), E_{pc} = −1.39 to −1.45 V) at 100 mVs^{-1} scan rate (Figure 7).[69] We performed cyclic voltammetry studies of **1-Ce^{TMS}** and **1-Ce^{Ph}** under similar conditions (Figure 7A). Reduction features were observed for **1-Ce^{TMS}** at E_{pc} = −1.66 V vs Fc/Fc^+ and **1-Ce^{Ph}** at E_{pc} = −1.58 V. The E_{pc} values compared [Ce(TriNOx)][OTf] (E_{pc} = −1.04 V) with outer-sphere OTf^- ligand, indicate inner-sphere coordination of the cerium alkynyl in solution in both cases.

The relatively negative E_{pc} values of the cerium(IV) alkynyl complexes indicate the strong electron donating character of the alkynyl ligand, notably stronger than that of the fluoride ligand, with an □0.2 V more negative redox potential. It should be noted that although the cerium(IV) imido complexes have a E_{pc} values less negative than the alkynyl analogues: [$M(L)_x$][Ce(TriNOx)=N-Ar] (-Ar = -(3,5-$(CF_3)_2C_6H_3$), E_{pc} = −1.39 to −1.45 V), this observation is likely due to the reduction of the imido ligand instead of cerium(IV) cation. Indeed, the imido ligand is a better electron-donating ligand, as indicated in the *trans*-influence section, *vide infra*. In comparison, they have a similar reduction potential with [Li(THF)$_4$][Ce(κ^2-ortho-oxa)(MBP)$_2$],[26] while the [Ce^{IV}(Alkyl)(NP(tert-butyl)$_3$)$_3$] has a much more negative reduction potential (−2.55 V - −2.92 V) due to the strong electron donating –N=P(tert-butyl) moiety in addition to alkyl ligand.[27] In general, these electrochemical data provide supporting evidence for a strong interaction between the Ce(IV) cation and –C≡C–R moieties (–R = $–SiMe_3$ or –Ph).

Reduction waves (E_{pc}) for **1-Ce^{TMS}** and **1-Ce^{Ph}** demonstrate the reduction of the Ce(IV) alkynyl complexes to corresponding Ce(III) moieties (Figure 7A, Table 2). However, this process is largely irreversible due to an accompanying chemical process. In this process, the reduced species, [Ce^{III}(C≡C–R)(TriNOx)]$^-$ is not stable and the alkynyl ligand presumably dissociates under the electrochemical conditions employed, similar to reported results for [Ce^{III}Cl(TriNOx)]$^-$.[29] Following the cathodic features for **1-Ce^{TMS}** and **1-Ce^{Ph}**, the subsequent anodic sweeps (E_{pa}) indicate the oxidation of the newly generated Ce(III) species, likely "[Ce^{III}(TriNOx)]", based on the observed oxidation potential and comparison with our previous results.[29]

Table 2. Cerium (III/IV) redox potential. [Ce^{IV}(TriNOx)]$^+$ derivatives, several common Ce^{IV} complexes, and several Ce^{IV}–C complexes from the literature are shown for comparison. a) E_p stands for redox potential from differential pulse voltammetry (DPV) instead of $E_{1/2}$. b) The scan rate was unknown, while other E_{pc} were measured at 100 mV/s scan rate.

Complex	E_{pc}	$E_{1/2}$
[Ce(TriNOx)](OTf)	−1.04 V	−0.95 V
[Ce(TriNOx)]I	−1.04 V	\
[Ce(TriNOx)Br]	−1.16 V (−1.04 V)	\
[Ce(TriNOx)Cl]	−1.26 V	\
[Ce(TriNOx)F]	−1.40 V	−1.36 V
[M][Ce(TriNOx)=NAr]	−1.39 V - −1.45 V	\
[Ce(TriNOx)(C≡CPh)]	**−1.58 V**	**−1.49 V (E_p)[a]**
[Ce(TriNOx)(C≡CTMS)]	**−1.66 V**	**−1.57 V (E_p)[a]**
[N^nBu_4]$_2$[Ce(NO_3)$_6$]	\	0.62 V
[$CeCl_6$]$^{2-}$	\	0.03 V
[Ce[N($SiMe_3$)$_2$]$_3$Cl]		−0.30 V
[Ce(COT)$_2$]	\	−1.40 V
[Ce(BIPM^{TMS})$_2$]	\	−1.63 V
[Li(THF)$_4$][Ce(κ^2-ortho-oxa)(MBP)$_2$]	−1.67 V	\
[Ce^{IV}(Alkyl)(NP(tert-butyl)$_3$)$_3$]	−2.55 V - −2.92 V[b]	\

View Article Online
DOI: 10.1039/D5SC03222A

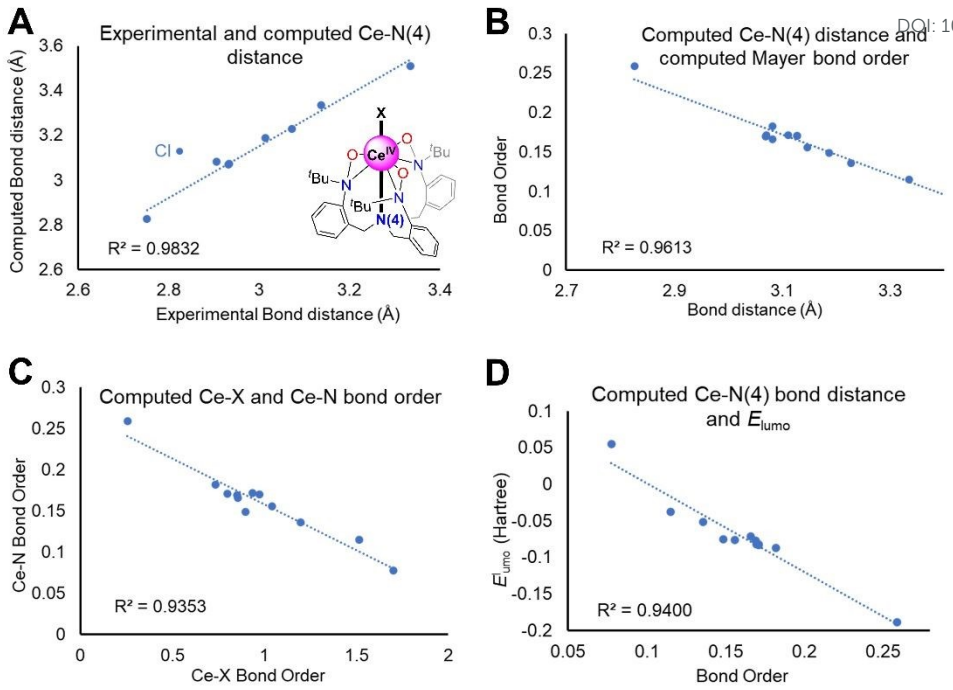

Fig. 8 *Trans*-influence on [Ce(TriNOx)(X)] complexes. **A**) Experimental and computed Ce-N(4) distance (Cl was excluded as an outlier). **B**) Computed Ce-N(4) distance and Mayer bond order. **C**) Computed Ce-X bond order and Ce-N(4) bond order. **D**) Computed Ce-N(4) bond distance and LUMO energy correlation.

Differential pulse voltammetry (DPV) experiments[70] were also used to determine potential values for the redox processes of **1-Ce^{TMS}** and **1-Ce^{Ph}**, where E_p = −1.57 V for **1-Ce^{TMS}**, −1.49 V for **1-Ce^{Ph}** vs Fc/Fc$^+$ (Figure 7B), for comparison with the measured $E_{1/2}$ values (**Table 2**).[29,71] These observed E_p values are more negative than some commonly observed cerium(IV) complexes, and are comparable with other organo-cerium(IV) complexes such as [Ce(COT)$_2$] or [Ce^{IV}(BIPM^{TMS})$_2$].[2, 3, 14]

Observation of a *Trans*-influence in the [Ce^{IV}X(TriNOx)] Series

The *trans*-influence is a structural phenomenon where a ligand bonded to a metal center weakens the bond of the metal to a second ligand located in the trans position. The structural *trans*-influence is well established for transition metal complexes,[72, 73] especially for heavy, late transition metals. Some reports, typically structural ones, have also been offered on the *trans*-influence in lanthanide(III) complexes.[74-77] Conversely, the *inverse-trans*-influence has been described in high oxidation state actinides complexes,[3, 42, 43, 78-83] where a ligand in a complex strengthens, rather than weakens, the bond of the ligand trans to it. And our group has studied this phenomenon in uranium(V, VI) chemistry previously.[42, 43, 81] However, there are open questions on the appearance of a *trans*-influence or *inverse-trans*-influence in cerium(IV) complexes, where few studies have been conducted. The Liddle group has discussed the possibility of an *inverse-trans*-influence in the tetravalent cerium(IV) phosphoimido complexes,[3] but the influence(s) at cerium(IV) requires additional study with a broad series of compounds.

Table 3. Data relevant to computational studies on *trans*-influence. The data includes Ce-N(4) computed distance, Ce-X and Ce-N(4) Mayer bond orders, and LUMO energy.

Axial Ligand X to [Ce(TriNOx)]$^+$	Computed Distance (Å)	Bond Order		Energy
	Ce-N(4)	Ce-X	Ce-N(4)	E_{LUMO} (Hartree)
THF	2.826	0.2564	0.2590	-0.1884
I$^-$	3.082	0.7353	0.1821	-0.0873
Br$^-$	3.111	0.9373	0.1712	-0.0820
Cl$^-$	3.129	0.9726	0.1695	-0.0821
F$^-$	3.147	1.0430	0.1559	-0.0767
$^-$C≡C-Ph	3.082	0.8552	0.1660	-0.0710
$^-$C≡C-TMS	3.069	0.8506	0.1691	-0.0772
$^-$NHAr	3.071	0.7999	0.1711	-0.0831
$^-$OSiPh$_3$	3.187	0.8972	0.1485	-0.0758
=NAr Li(TMEDA)	3.228	1.1970	0.1359	-0.0520
=NAr K(DME)$_2$	3.335	1.5158	0.1151	-0.0383
=NAr [Cs(Cryptand)]	3.510	1.7020	0.0774	0.0550

In the current work, a *trans*-position has been studied for the current and previously reported, structurally conserved [Ce^{IV}(TriNOx)X] complexes, considering the axial nitrogen atom N(4) from the tridentate $TriNOx^{3-}$ ligand and terminal X^- (or L) ligand (Figure 8). For example, X^- in **1-Ce^{TMS}**/**1-Ce^{Ph}** indicates the alkynyl ligands. The angles of X-Ce-N(4)$_{TriNOx}$ of the complexes range from 173.8(3)º to 179.34(8)º in the crystal structures, and range from 172.84º to 179.98º in the DFT optimized structures, indicating the validity for the *trans*-position of X^- and N(4) atoms on the cerium atom. A series of X^- (or L) ligands for the complexes have been compared from weakly coordinating to strongly coordinating: -THF, -halide (iodide, bromide, chloride, fluoride), -alkynyl, -anilide, -siloxide, -imide (Li-capped, K-capped and uncapped imides) (See supporting information). The Ce(IV)-N(4) bonding interaction is understood to be weak but nevertheless important and diagnostic metric on axial bonding in this system. It should be noted that, in the solution phase, the iodide ligand is outer-sphere, and bromide ligand is partially outer-sphere (in chemical equilibrium between inner- and outer-sphere). But those two ligands, I^- and Br^-, were considered inner sphere for the structures considered in this study. The complexes were ranked by increasing Ce-N(4) distance, excepting the halides. Among halides complexes [Ce^{IV}(TriNOx)X, X = F^-, Cl^-, Br^-, I^-], only the Cl^- complex was previously characterized by crystallography, while the rest were characterized by elemental analysis and NMR.[29] Here, all the halide complexes were used as model complexes for computational studies. It also should be noted that these computational studies on the *trans*-influence use similar methods, with the B3LYP hybrid functional and 6-31G(d) basis set, as those in previous studies on the [Ce^{IV}(TriNOx)X] system, for consistency.[29]

We posited that the most telling case for the *trans* influence in the current system would be made with multiple lines of experimental and computational metrics that incorporate X-ray structural and computational electronic structural aspects concurrently (Figure 8).[43] The computational methods undertaken here are different from those described in previous sections of the current work and a description of the trans influence computational study is also provided in the supporting information. As described before,[29] the accuracy between the computed distance of Ce-O$_{TriNOx}$ and experimental result indicates an acceptable computational model performance. The Ce-X distances exhibit a good correlation between the experimental and computed results, with differences less than 0.08 Å, except for the chloride complex (0.12 Å). The Ce-N(4)$_{TriNOx}$ distances also demonstrated reasonable agreement between experimental and computed values, except chloride (Figure 8A). We also observed a negative correlation between computed Ce-N(4) bond distance and Mayer bond order (Figure 8B), consistent with a stronger bond with a shorter distance.

Mayer bond order has been used to compare the halide derivatives of the [Ce^{IV}(TriNOx)X] complexes.[29] Based on the computational results in Figure 8C, it is evident that, a larger Mayer bond order of Ce-X (or L), exhibits a *trans*-influence and results in a smaller Mayer bond orders of Ce–N(4), indicating a stronger donating ability of X/L ligand on cerium result in a weaker bond between Ce and N(4). The LUMO orbital of these complexes primarily consist of 4f character and the LUMO energies are correlated to the electron donating ability of the ligands.[84] We observe a similar trend between the LUMO energy and Ce-N(4) distance, where a stronger Ce-X bond and longer but weaker Ce-N(4) bond result in a higher LUMO energy (Figure 8D), similar to previous observation.[29]

To better illustrate the *trans*-influence, this phenomenon can be interpreted using the Ce-N(4) experimental bond distances (Table S1). Weakly coordinated THF resulted in a Ce-N(4) bond length of 2.717(9)-2.787(8) Å and the chloride (Cl^-) ligand resulted in a Ce-N(4) bond length of 2.825(3) Å. The relatively strongly sigma-donating alkynyl ligands yielded a Ce-N(4) bond length of 2.906(2) Å for [Ce(TriNOx)(C≡C-Ph)], and 2.932 Å for [Ce(TriNOx)(C≡C-TMS)], whereas the anilide ligand resulted in bond length of 2.934(3) Å for [Ce(TriNOx)(NHAr)] (Ar = (3,5-$(CF_3)_2C_6H_3$). Thus, notably, the alkynyl ligand exhibits a strong donating ability comparable to that of the anilide ligand, indicating a stronger bonding interaction between cerium and alkynyl moiety (see supporting information). By way of comparison, the extraordinarily strongly-coordinating uncapped imido ligand gives a bond distance of 3.335 Å for Ce-N(4) of [Cs(2.2.2-cryptand)][Ce(TriNOx)(NAr)]. To conclude, the bond distance and bond order well-reflects the bonding interactions of the Ce-X and Ce-N(4) moieties and illustrate a structural *trans*-influence is operative in this series.

Conclusions and Outlook

The synthesis and characterization of cerium(IV)/thorium(IV) alkynyl complexes, **1-Ce^{Ph}**, **1-Ce^{TMS}**, **1-Th^{TMS}** have expanded the understanding of cerium/throium-carbon bonding by providing insights into their structural, spectroscopic, and electrochemical properties. These studies reveal the unique covalent contributions of Ce 5d- and 4f-orbitals in M–C bonding interactions, as evidenced by X-ray crystallography, Raman spectroscopy, and ^{13}C NMR spectroscopy chemical shifts. Comparative analyses with thorium(IV) analogues and other cerium(IV) complexes highlight the strong electron-donating nature of alkynyl ligands, resulting in notable redox properties. Furthermore, these findings challenge traditional notions of f-element bonding, by emphasizing the significant covalency in Ce(IV)-carbon bonds and the influence of spin-orbit coupling effects. The observed *trans*-influence in the [Ce^{IV}(TriNOx)X] framework enriches our understanding of ligand-field effects in high oxidation state lanthanide complexes, and offers a foundation for future studies on bonding and possibly unique reactivity in f-block chemistry.

Author contributions

Q.Y. proposed and synthesized **1-Ce^{TMS}**, **1-Ce^{Ph}**, conducted NMR, electrochemistry, UV-Vis, *trans*-influence studies and drafted an initial manuscript draft. Q.Y. and E. L. synthesized **1-Th^{TMS}**. X. Y. and J. A. conducted the computational analysis for **1-Ce^{TMS}**, **1-Ce^{Ph}** and **1-Th^{TMS}** and supervised the *trans*-influence aspects of the work. P.P. and Q.Y. conducted the Raman and IR studies. P.P. conducted elemental analysis of the three complexes reported. P.W.S., and S.G.M. conducted the XAS studies. H.G. conducted the magnetism studies with Q.Y. taking part. Q.Y., E.L., X.Y., J.A. and E.J.S. wrote the manuscript. All co-authors participated in the revisions. M.R.G. and P. J. C. resolved the crystal structures. E.J.S. supervised all aspect of the project.

Conflicts of interest

There are no conflicts to declare.

Data availability

The data supporting this article have been included as part of the Supplementary Information. Crystallographic data for **1-Ce^{TMS}, 1-Ce^{Ph} and 1-Th^{TMS}** have been deposited at the CCDC under 2448118-2448120, and can be obtained from https://www.ccdc.cam.ac.uk/structures/

Acknowledgements

Q.Y. thanks Dr. Bren E. Cole for his mentorship, support and assistance on [Ce(TriNOx)Cl] synthesis. E.J.S. thanks the U.S. National Science Foundation (CHE-2247668) for financial support of this work. E.J.S. also thanks the University of Pennsylvania for support. This work was supported at Lawrence Berkeley National Laboratory by Director, Office of Science, Office of Basic Energy Sciences, Division of Chemical Sciences, Geosciences, and Biosciences Heavy Element Chemistry (HEC) program of the United States Department of Energy (DOE) under contract DE-AC02-05CH11231. We also thank JASCO for use of Raman instrumentation in the JASCO facility for Spectroscopic Excellence in the Chemistry Department at the University of Pennsylvania.

Notes and references

(1) Neidig, M. L.; Clark, D. L.; Martin, R. L. Covalency in f-element complexes. *Coord. Chem. Rev.* **2013**, *257* (2), 394-406.
(2) Panetti, G. B.; Sergentu, D.-C.; Gau, M. R.; Carroll, P. J.; Autschbach, J.; Walsh, P. J.; Schelter, E. J. Isolation and characterization of a covalent CeIV-Aryl complex with an anomalous 13C chemical shift. *Nat. Commun.* **2021**, *12* (1), 1713. DOI: 10.1038/s41467-021-21766-4.
(3) Gregson, M.; Lu, E.; Mills, D. P.; Tuna, F.; McInnes, E. J. L.; Hennig, C.; Scheinost, A. C.; McMaster, J.; Lewis, W.; Blake, A. J.; et al. The inverse-trans-influence in tetravalent lanthanide and actinide bis(carbene) complexes. *Nat. Commun.* **2017**, *8* (1), 14137. DOI: 10.1038/ncomms14137.
(4) Cheisson, T.; Schelter, E. J. Rare earth elements: Mendeleev's bane, modern marvels. *Science* **2019**, *363* (6426), 489-493. DOI: doi:10.1126/science.aau7628.
(5) Pandey, P.; Yang, Q.; Gau, M. R.; Schelter, E. J. Evaluating the photophysical and photochemical characteristics of green-emitting cerium(iii) mono-cyclooctatetraenide complexes. *Dalton Trans.* **2023**, *52* (18), 5909-5917. DOI: 10.1039/D3DT00351E.
(6) Moreau, L. M.; Lapsheva, E.; Amaro-Estrada, J. I.; Gau, M. R.; Carroll, P. J.; Manor, B. C.; Qiao, Y.; Yang, Q.; Lukens, W. W.; Sokaras, D.; et al. Electronic structure studies reveal 4f/5d mixing and its effect on bonding characteristics in Ce-imido and -oxo complexes. *Chem. Sci.* **2022**, *13* (6), 1759-1773. DOI: 10.1039/D1SC06623D.
(7) Autschbach, J. The role of the exchange-correlation response kernel and scaling corrections in relativistic density functional nuclear magnetic shielding calculations with the zeroth-order regular approximation. *Mol. Phys.* **2013**, *111* (16-17), 2544-2554. DOI: 10.1080/00268976.2013.796415.
(8) Gilge, J. W.; Roesky, H. W. Structurally Characterized Organometallic Hydroxo Complexes of the f- and d-Block Metals. *Chem. Rev.* **1994**, *94* (4), 895-910. DOI: 10.1021/cr00028a003.
(9) Yang, Q.; Wang, Y.-H.; Qiao, Y.; Gau, M.; Carroll, P. J.; Walsh, P. J.; Schelter, E. J. Photocatalytic C-H activation and the subtle role of chlorine radical complexation in reactivity. *Science* **2021**, *372* (6544), 847-852. DOI: doi:10.1126/science.abd8408.
(10) Yang, Q.; Song, E.; Wu, Y.; Li, C.; Gau, M. R.; Anna, J. M.; Schelter, E. J.; Walsh, P. J. Mechanistic Investigation of the Ce(III) Chloride Photoredox Catalysis System: Understanding the Role of Alcohols as Additives. *J. Am. Chem. Soc.* **2025**. DOI: 10.1021/jacs.4c15627.
(11) Lapsheva, E.; Yang, Q.; Cheisson, T.; Pandey, P.; Carroll, P. J.; Gau, M.; Schelter, E. J. Electronic Structure Studies and Photophysics of Luminescent Th(IV) Anilido and Imido Complexes. *Inorg. Chem.* **2023**, *62* (15), 6155-6168. DOI: 10.1021/acs.inorgchem.3c00375.
(12) Solola, L. A.; Zabula, A. V.; Dorfner, W. L.; Manor, B. C.; Carroll, P. J.; Schelter, E. J. An Alkali Metal-Capped Cerium(IV) Imido Complex. *J. Am. Chem. Soc.* **2016**, *138* (22), 6928-6931. DOI: 10.1021/jacs.6b03293.
(13) Solola, L. A.; Zabula, A. V.; Dorfner, W. L.; Manor, B. C.; Carroll, P. J.; Schelter, E. J. Cerium (IV) imido complexes: structural, computational, and reactivity studies. *J. Am. Chem. Soc.* **2017**, *139* (6), 2435-2442.
(14) Gregson, M.; Lu, E.; McMaster, J.; Lewis, W.; Blake, A. J.; Liddle, S. T. A Cerium(IV)–Carbon Multiple Bond. *Angew. Chem. Int. Ed.* **2013**, *52* (49), 13016-13019. DOI: https://doi.org/10.1002/anie.201306984.
(15) Walter, M. D.; Booth, C. H.; Lukens, W. W.; Andersen, R. A. Cerocene Revisited: The Electronic Structure of and Interconversion Between Ce2(C8H8)3 and Ce(C8H8)2. *Organometallics* **2009**, *28* (3), 698-707. DOI: 10.1021/om7012327.
(16) Choppin, G. R. Covalency in f-element bonds. *J. Alloys Compd.* **2002**, *344* (1-2), 55-59.
(17) Yang, Q.; Qiao, Y.; McSkimming, A.; Moreau, L. M.; Cheisson, T.; Booth, C. H.; Lapsheva, E.; Carroll, P. J.; Schelter, E. J. A hydrolytically stable Ce(iv) complex of glutarimide-dioxime. *Inorg. Chem. Front.* **2021**, *8* (4), 934-939. DOI: 10.1039/D0QI00969E.
(18) Yang, Q. Organometallic and Photochemistry of Cerium and Thorium Complexes and Photocatalytic Systems for the Generation of Chlorine Radicals. University of Pennsylvania, 2022.
(19) Evans, W. J.; Deming, T. J.; Ziller, J. W. The utility of ceric ammonium nitrate-derived alkoxide complexes in the synthesis of organometallic cerium(IV) complexes. Synthesis and first x-ray crystallographic determination of a tetravalent cerium

cyclopentadienide complex, (C5H5)3Ce(OCMe3). *Organometallics* **1989**, *8* (6), 1581-1583. DOI: 10.1021/om00108a042.
(20) Dröse, P.; Crozier, A. R.; Lashkari, S.; Gottfriedsen, J.; Blaurock, S.; Hrib, C. G.; Maichle-Mössmer, C.; Schädle, C.; Anwander, R.; Edelmann, F. T. Facile Access to Tetravalent Cerium Compounds: One-Electron Oxidation Using Iodine(III) Reagents. *J. Am. Chem. Soc.* **2010**, *132* (40), 14046-14047. DOI: 10.1021/ja107494h.
(21) Kerridge, A. Oxidation state and covalency in f-element metallocenes (M = Ce, Th, Pu): a combined CASSCF and topological study. *Dalton Trans.* **2013**, *42* (46), 16428-16436. DOI: 10.1039/C3DT52279B.
(22) Streitwieser, A.; Kinsley, S. A.; Jenson, C. H.; Rigsbee, J. T. Synthesis and Properties of Di-π-[8]annulenecerium(IV), Cerocene. *Organometallics* **2004**, *23* (22), 5169-5175. DOI: 10.1021/om049743+.
(23) Greco, A.; Cesca, S.; Bertolini, W. New 7r-cyclooctate'I'raenyl and iT-cyclopentadienyl complexes of cerium. *J. Organomet. Chem.* **1976**, *113* (4), 321-330. DOI: https://doi.org/10.1016/S0022-328X(00)96143-6.
(24) Balazs, G.; Cloke, F. G. N.; Green, J. C.; Harker, R. M.; Harrison, A.; Hitchcock, P. B.; Jardine, C. N.; Walton, R. Cerium(III) and Cerium(IV) Bis(η8-pentalene) Sandwich Complexes: Synthetic, Structural, Spectroscopic, and Theoretical Studies. *Organometallics* **2007**, *26* (13), 3111-3119. DOI: 10.1021/om7002738.
(25) Casely, I. J.; Liddle, S. T.; Blake, A. J.; Wilson, C.; Arnold, P. L. Tetravalent cerium carbene complexes. *Chem. Commun.* **2007**, (47), 5037-5039, 10.1039/B713041D. DOI: 10.1039/B713041D.
(26) Feng, B.; Ye, L.-W.; Wang, N.; Hu, H.-S.; Li, J.; Tamm, M.; Chen, Y. Endeavoring Cerium (IV)-Alkyl,-Aryl and-Alkynyl Complexes by an Energy-Level Match Strategy. *CCS Chem.* **2025**, *7* (4), 1043-1053. DOI: 10.31635/ccschem.024.202404131.
(27) Tateyama, H.; Boggiano, A. C.; Liao, C.; Otte, K. S.; Li, X.; La Pierre, H. S. Tetravalent Cerium Alkyl and Benzyl Complexes. *J. Am. Chem. Soc.* **2024**, *146* (15), 10268-10273.
(28) Vincenzini, B. D.; Yu, X.; Paloc, S.; Smith, P. W.; Gupta, H.; Pandey, P.; Kent, G. T.; Ordonez, O.; Keller, T.; Gau, M. R.; et al. 4f-orbital covalency enables a single-crystal-to-single-crystal ring-opening isomerization in a CeIV–cyclopropenyl complex. *Nature Chemistry* **2025**. DOI: 10.1038/s41557-025-01791-2.
(29) Bogart, J. A.; Lippincott, C. A.; Carroll, P. J.; Booth, C. H.; Schelter, E. J. Controlled Redox Chemistry at Cerium within a Tripodal Nitroxide Ligand Framework. *Chem. - Eur. J.* **2015**, *21* (49), 17850-17859. DOI: https://doi.org/10.1002/chem.201502952.
(30) Lapsheva, E. N.; Cheisson, T.; Álvarez Lamsfus, C.; Carroll, P. J.; Gau, M. R.; Maron, L.; Schelter, E. J. Reactivity of Ce(iv) imido compounds with heteroallenes. *Chem. Commun.* **2020**, *56* (35), 4781-4784. DOI: 10.1039/C9CC10052K.
(31) Maynadié, J.; Berthet, J.-C.; Thuéry, P.; Ephritikhine, M. Cyanide metallocenes of trivalent f-elements. *Organometallics* **2007**, *26* (10), 2623-2629.
(32) Schneider, D.; Anwander, R. Pentamethylcyclopentadienyl-Supported Cerocene(III) Complexes. *Eur. J. Inorg. Chem.* **2017**, *2017* (8), 1180-1188. DOI: https://doi.org/10.1002/ejic.201601404.
(33) Kim, J. E.; Weinberger, D. S.; Carroll, P. J.; Schelter, E. J. Synthesis, Structural Characterization, and Carbonyl Addition Reactivity of a Terminal Cerium (III) Acetylide Complex. *Organometallics* **2014**, *33* (21), 5948-5951.
(34) Shannon, R. D. Revised effective ionic radii and systematic studies of interatomic distances in halides and chalcogenides. *Acta Crystallogr. Sec. A* **1976**, *32* (5), 751-767.
(35) Garner, M. E.; Parker, B. F.; Hohloch, S.; Bergman, R. G.; Arnold, J. Thorium Metallacycle Facilitates Catalytic Alkyne Hydrophosphination. *J. Am. Chem. Soc.* **2017**, *139* (37), 12935-12938. DOI: 10.1021/jacs.7b08323.
(36) Suvova, M.; O'Brien, K. T. P.; Farnaby, J. H.; Love, J. B.; Kaltsoyannis, N.; Arnold, P. L. Thorium(IV) and Uranium(IV) trans-Calix[2]benzene[2]pyrrolide Alkyl and Alkynyl Complexes: Synthesis, Reactivity, and Electronic Structure. *Organometallics* **2017**, *36* (23), 4669-4681. DOI: 10.1021/acs.organomet.7b00633.
(37) Settineri, N. S.; Arnold, J. Insertion, protonolysis and photolysis reactivity of a thorium monoalkyl amidinate complex. *Chem. Sci.* **2018**, *9* (10), 2831-2841. DOI: 10.1039/C7SC05328B.
(38) Wang, Y.; Zhang, C.; Zi, G.; Ding, W.; Walter, M. D. Preparation of a potassium chloride bridged thorium phosphinidiide complex and its reactivity towards small organic molecules. *New J. Chem.* **2019**, *43* (24), 9527-9539. DOI: 10.1039/C9NJ02269D.
(39) Kent, G. T.; Yu, X.; Pauly, C.; Wu, G.; Autschbach, J.; Hayton, T. W. Synthesis of Parent Acetylide and Dicarbide Complexes of Thorium and Uranium and an Examination of Their Electronic Structures. *Inorg. Chem.* **2021**, *60* (20), 15413-15420. DOI: 10.1021/acs.inorgchem.1c02064.
(40) Vícha, J.; Novotný, J.; Komorovsky, S.; Straka, M.; Kaupp, M.; Marek, R. Relativistic Heavy-Neighbor-Atom Effects on NMR Shifts: Concepts and Trends Across the Periodic Table. *Chem. Rev.* **2020**, *120* (15), 7065-7103. DOI: 10.1021/acs.chemrev.9b00785.
(41) Hayton, T. W.; Autschbach, J. Using NMR Spectroscopy to Evaluate Metal–Ligand Bond Covalency for the f Elements. *Acc. Chem. Res.* **2025**, *58* (3), 488-498. DOI: 10.1021/acs.accounts.4c00727.
(42) Mullane, K. C.; Hrobárik, P.; Cheisson, T.; Manor, B. C.; Carroll, P. J.; Schelter, E. J. 13C NMR Shifts as an Indicator of U–C Bond Covalency in Uranium(VI) Acetylide Complexes: An Experimental and Computational Study. *Inorg. Chem.* **2019**, *58* (7), 4152-4163. DOI: 10.1021/acs.inorgchem.8b03175.
(43) Lewis, A. J.; Carroll, P. J.; Schelter, E. J. Stable Uranium(VI) Methyl and Acetylide Complexes and the Elucidation of an Inverse Trans Influence Ligand Series. *J. Am. Chem. Soc.* **2013**, *135* (35), 13185-13192. DOI: 10.1021/ja406610r.
(44) Ordoñez, O.; Yu, X.; Wu, G.; Autschbach, J.; Hayton, T. W. Homoleptic Perchlorophenyl "Ate" Complexes of Thorium(IV) and Uranium(IV). *Inorg. Chem.* **2021**, *60* (16), 12436-12444. DOI: 10.1021/acs.inorgchem.1c01686.
(45) Ordoñez, O.; Yu, X.; Wu, G.; Autschbach, J.; Hayton, T. W. Synthesis and Characterization of Two Uranyl-Aryl "Ate" Complexes. *Chem. - Eur. J.* **2021**, *27* (19), 5885-5889. DOI: https://doi.org/10.1002/chem.202005078.
(46) Seaman, L. A.; Hrobárik, P.; Schettini, M. F.; Fortier, S.; Kaupp, M.; Hayton, T. W. A Rare Uranyl(VI)–Alkyl Ate Complex [Li(DME)1.5]2[UO2(CH2SiMe3)4] and Its Comparison with a Homoleptic Uranium(VI)–Hexaalkyl. *Angew. Chem. Int. Ed.* **2013**, *52* (11), 3259-3263. DOI: https://doi.org/10.1002/anie.201209611.
(47) Pedrick, E. A.; Hrobárik, P.; Seaman, L. A.; Wu, G.; Hayton, T. W. Synthesis, structure and bonding of hexaphenyl thorium(iv): observation of a non-octahedral structure. *Chem. Commun.* **2016**, *52* (4), 689-692. DOI: 10.1039/C5CC08265J.
(48) Seaman, L. A.; Pedrick, E. A.; Tsuchiya, T.; Wu, G.; Jakubikova, E.; Hayton, T. W. Comparison of the Reactivity of 2-Li-C6H4CH2NMe2 with MCl4 (M=Th, U): Isolation of a Thorium Aryl Complex or a Uranium Benzyne Complex. *Angew. Chem. Int. Ed.* **2013**, *52* (40), 10589-10592. DOI: https://doi.org/10.1002/anie.201303992.
(49) Hrobárik, P.; Hrobáriková, V.; Greif, A. H.; Kaupp, M. Giant Spin-Orbit Effects on NMR Shifts in Diamagnetic Actinide Complexes: Guiding the Search of Uranium(VI) Hydride Complexes in the Correct

Spectral Range. *Angew. Chem. Int. Ed.* **2012**, *51* (43), 10884-10888. DOI: https://doi.org/10.1002/anie.201204634.
(50) Starkey, L. S. *13C NMR Chemical Shifts*. https://www.cpp.edu/~lsstarkey/courses/NMR/NMRshifts13C.pdf (accessed.
(51) Pandey, P.; Yu, X.; Panetti, G. B.; Lapsheva, E.; Gau, M. R.; Carroll, P. J.; Autschbach, J.; Schelter, E. J. Synthesis, Electrochemical, and Computational Studies of Organocerium(III) Complexes with Ce–Aryl Sigma Bonds. *Organometallics* **2023**, *42* (12), 1267-1277. DOI: 10.1021/acs.organomet.2c00384.
(52) Wilson, H. H.; Yu, X.; Cheisson, T.; Smith, P. W.; Pandey, P.; Carroll, P. J.; Minasian, S. G.; Autschbach, J.; Schelter, E. J. Synthesis and Characterization of a Bridging Cerium(IV) Nitride Complex. *J. Am. Chem. Soc.* **2023**, *145* (2), 781-786. DOI: 10.1021/jacs.2c12145.
(53) Cheisson, T.; Kersey, K. D.; Mahieu, N.; McSkimming, A.; Gau, M. R.; Carroll, P. J.; Schelter, E. J. Multiple Bonding in Lanthanides and Actinides: Direct Comparison of Covalency in Thorium(IV)- and Cerium(IV)-Imido Complexes. *J. Am. Chem. Soc.* **2019**, *141* (23), 9185-9190. DOI: 10.1021/jacs.9b04061.
(54) Gremillion, A. J.; Ross, J.; Yu, X.; Ishtaweera, P.; Anwander, R.; Autschbach, J.; Baker, G. A.; Kelley, S. P.; Walensky, J. R. Facile Oxidation of Ce(III) to Ce(IV) Using Cu(I) Salts. *Inorg. Chem.* **2024**, *63* (21), 9602-9609. DOI: 10.1021/acs.inorgchem.3c04337.
(55) Ordoñez, O.; Yu, X.; Wu, G.; Autschbach, J.; Hayton, T. W. Assessing the 4f Orbital Participation in the Ln–C Bonds of [Li(THF)4][Ln(C6Cl5)4] (Ln = La, Ce). *Inorg. Chem.* **2022**, *61* (38), 15138-15143. DOI: 10.1021/acs.inorgchem.2c02304.
(56) Rodionov, A. N.; Timofeyuk, G. V.; Talalaeva, T. V.; Shigorin, D. N.; Kocheshkov, K. A. Infrared spectra of some acetylides of lithium, sodium, and potassium. *Bull. Acad. Sci. USSR, Div. Chem. Sci.* **1965**, *14* (1), 37-40. DOI: 10.1007/BF00854856.
(57) Pellny, P.-M.; Kirchbauer, F. G.; Burlakov, V. V.; Baumann, W.; Spannenberg, A.; Rosenthal, U. Reactivity of Permethylzirconocene and Permethyltitanocene toward Disubstituted 1, 3-Butadiynes: η4- vs η2-Complexation or C− C Coupling with the Permethyltitanocene. *J. Am. Chem. Soc.* **1999**, *121* (36), 8313-8323.
(58) Lee, K. E.; Higa, K. T.; Nissan, R. A.; Butcher, R. J. Synthesis, characterization, and structure of acetylenic gallium dialkylphosphides having the formula [(tert-Bu)(Me3SiC. tplbond. C) GaPR2] 2 (R= Et, iso-Pr, tert-Bu). *Organometallics* **1992**, *11* (8), 2816-2821.
(59) Lang, H.; Seyferth, D. Synthese und Reaktivität von Alkinyl-substituierten Titanocen-Komplexen/Synthesis and Reactivity of Alkyne Substituted Titanocene Complexes. *Z. Naturforsch. B* **1990**, *45* (2), 212-220.
(60) Lorberth, J. Spaltung der zinn-stickstoffbindung: (phenylalkynyl)stannane. *J. Organomet. Chem.* **1969**, *16* (2), 327-331. DOI: https://doi.org/10.1016/S0022-328X(00)81124-9.
(61) Jeffery, E.; Mole, T. Some new associated (phenylethynyl) metallic and octynylmetallic compounds. *J. Organomet. Chem.* **1968**, *11*, 393-398.
(62) Lee, K. E.; Higa, K. T. Synthesis, characterization, and reactivity of new alkylgallium acetylides. *J. Organomet. Chem.* **1993**, *449* (1-2), 53-59.
(63) Deacon, G.; Wilkinson, D. Organolanthanoids. XII. Reactions of bis (cyclopentadienyl) ytterbium (II) with some diorganomercurials. *Inorg. Chim. Acta* **1988**, *142* (1), 155-159.
(64) Dolzine, T.; Hovland, A.; Oliver, J. Intramolecular cyclization of dimethyl (1-pent-4-enyl)-silyllithium. *J. Organomet. Chem.* **1974**, *65* (1), C1-C3.
(65) Seavill, P. W.; Holt, K. B.; Wilden, J. D. Electrochemical preparation and applications of copper (i) acetylides: a demonstration of how electrochemistry can be used to facilitate sustainability in homogeneous catalysis. *Green Chem.* **2018**, *20* (24), 5474-5478.
(66) Branson, J. A.; Smith, P. W.; Sergentu, D.-C.; Russo, D. R.; Gupta, H.; Booth, C. H.; Arnold, J.; Schelter, E. J.; Autschbach, J.; Minasian, S. G. The Counterintuitive Relationship between Orbital Energy, Orbital Overlap, and Bond Covalency in CeF62– and CeCl62–. *J. Am. Chem. Soc.* **2024**, *146* (37), 25640-25655. DOI: 10.1021/jacs.4c07459.
(67) Qiao, Y.; Yin, H.; Moreau, L. M.; Feng, R.; Higgins, R. F.; Manor, B. C.; Carroll, P. J.; Booth, C. H.; Autschbach, J.; Schelter, E. J. Cerium(iv) complexes with guanidinate ligands: intense colors and anomalous electronic structures. *Chem. Sci.* **2021**, *12* (10), 3558-3567. DOI: 10.1039/D0SC05193D.
(68) Booth, C. H.; Walter, M. D.; Daniel, M.; Lukens, W. W.; Andersen, R. A. Self-Contained Kondo Effect in Single Molecules. *Phys. Rev. Lett.* **2005**, *95* (26), 267202. DOI: 10.1103/PhysRevLett.95.267202.
(69) The electrochemistry of [M][Ce(TriNOx)=N-(3,5-(CF3)2C6H3)] was measured in DME and the electrochemistry of Ce(TriNOx)-X was measured in DCM. The CeTMS and CePh in this article was measured in DCM.
(70) Sandford, C.; Edwards, M. A.; Klunder, K. J.; Hickey, D. P.; Li, M.; Barman, K.; Sigman, M. S.; White, H. S.; Minteer, S. D. A synthetic chemist's guide to electroanalytical tools for studying reaction mechanisms. *Chem. Sci.* **2019**, *10* (26), 6404-6422. DOI: 10.1039/C9SC01545K.
(71) The redox potential from DPV was obtained from the average of reduction and oxidation peak voltage.
(72) Appleton, T. G.; Clark, H. C.; Manzer, L. E. The trans-influence: its measurement and significance. *Coord. Chem. Rev.* **1973**, *10* (3), 335-422. DOI: https://doi.org/10.1016/S0010-8545(00)80238-6.
(73) Coe, B. J.; Glenwright, S. J. Trans-effects in octahedral transition metal complexes. *Coord. Chem. Rev.* **2000**, *203* (1), 5-80.
(74) Krogh-Jespersen, K.; Romanelli, M. D.; Melman, J. H.; Emge, T. J.; Brennan, J. G. Covalent Bonding and the Trans Influence in Lanthanide Compounds. *Inorg. Chem.* **2010**, *49* (2), 552-560. DOI: 10.1021/ic901571m.
(75) Deacon, G. B.; Forsyth, C. M. A Half-Sandwich Perfluoroorganoytterbium(II) Complex from a Simple Redox Transmetalation/Ligand Exchange Synthesis. *Organometallics* **2003**, *22* (7), 1349-1352. DOI: 10.1021/om021039a.
(76) Freedman, D.; Melman, J. H.; Emge, T. J.; Brennan, J. G. Cubane Clusters Containing Lanthanide Ions: (py)8Yb4Se4(SePh)4 and (py)10Yb6S6(SPh)6. *Inorg. Chem.* **1998**, *37* (17), 4162-4163. DOI: 10.1021/ic9805832.
(77) Deacon, G. B.; Feng, T. C.; Skelton, B. W.; White, A. H. Organoamido-and Aryloxo-Lanthanoids. XI. Syntheses and Crystal Structures of $Nd(Odpp)_3$, $Nd(Odpp)_3(thf)$ and $[Nd(Odpp)_3(thf)_2]$*2 (thf)(Odpp⁻=2, 6-Diphenylphenolate): Variations in Intramolecular π-Ph-Nd Interactions. *Aust. J. Chem.* **1995**, *48* (4), 741-756.
(78) O'Grady, E.; Kaltsoyannis, N. On the inverse trans influence. Density functional studies of [MOX5]n− (M = Pa, n = 2; M = U, n = 1; M = Np, n = 0; X = F, Cl or Br). *J. Chem. Soc., Dalton Trans.* **2002**, (6). DOI: 10.1039/B109696F.
(79) Lam, O. P.; Franke, S. M.; Nakai, H.; Heinemann, F. W.; Hieringer, W.; Meyer, K. Observation of the Inverse Trans Influence (ITI) in a Uranium(V) Imide Coordination Complex: An Experimental Study and Theoretical Evaluation. *Inorg. Chem.* **2012**, *51* (11), 6190-6199. DOI: 10.1021/ic300273d.
(80) La Pierre, H. S.; Rosenzweig, M.; Kosog, B.; Hauser, C.; Heinemann, F. W.; Liddle, S. T.; Meyer, K. Charge control of the inverse trans-influence. *Chem. Commun.* **2015**, *51* (93), 16671-16674.

View Article Online
DOI: 10.1039/D5SC03222A

(81) Lewis, A. J.; Mullane, K. C.; Nakamaru-Ogiso, E.; Carroll, P. J.; Schelter, E. J. The Inverse Trans Influence in a Family of Pentavalent Uranium Complexes. *Inorg. Chem.* **2014**, *53* (13), 6944-6953. DOI: 10.1021/ic500833s.
(82) Motta, L. C.; Autschbach, J. Actinide inverse trans influence versus cooperative pushing from below and multi-center bonding. *Nat. Commun.* **2023**, *14* (1), 4307. DOI: 10.1038/s41467-023-39626-8.
(83) La Pierre, H. S.; Meyer, K. Uranium–Ligand Multiple Bonding in Uranyl Analogues, [L═U═L]n+, and the Inverse Trans Influence. *Inorg. Chem.* **2013**, *52* (2), 529-539. DOI: 10.1021/ic302412j.
(84) Levin, J. R.; Dorfner, W. L.; Dai, A. X.; Carroll, P. J.; Schelter, E. J. Density Functional Theory as a Predictive Tool for Cerium Redox Properties in Nonaqueous Solvents. *Inorg. Chem.* **2016**, *55* (24), 12651-12659. DOI: 10.1021/acs.inorgchem.6b01779.

View Article Online
DOI: 10.1039/D5SC03222A

The data supporting this article have been included as part of the Supplementary Information. Crystallographic data for 1-Ce^{TMS}, 1-Ce^{Ph} and 1-Th^{TMS} have been deposited at the CCDC under [accession numbers] and can be obtained from https://www.ccdc.cam.ac.uk/structures/